

A new topology of resonant inverter including a piezoelectric component

Vincent Massavie, Ghislain Despesse, Sébastien Carcouet, Xavier Maynard

▶ **To cite this version:**

Vincent Massavie, Ghislain Despesse, Sébastien Carcouet, Xavier Maynard. A new topology of resonant inverter including a piezoelectric component. IEEE Access, 2021, pp.P.1-P.10. cea-03507090

HAL Id: cea-03507090
https://cea.hal.science/cea-03507090

Submitted on 3 Jan 2022

HAL is a multi-disciplinary open access archive for the deposit and dissemination of scientific research documents, whether they are published or not. The documents may come from teaching and research institutions in France or abroad, or from public or private research centers.

L'archive ouverte pluridisciplinaire **HAL**, est destinée au dépôt et à la diffusion de documents scientifiques de niveau recherche, publiés ou non, émanant des établissements d'enseignement et de recherche français ou étrangers, des laboratoires publics ou privés.

A new topology of resonant inverter including a piezoelectric component

MASSAVIE Vincent	DESPESSE Ghislain	CARCOUET Sebastien	MAYNARD Xavier
CEA-Leti,	CEA-Leti,	CEA-Leti,	CEA-Liten,
Université Grenoble	Université Grenoble	Université Grenoble	Université Grenoble
Alpes, F-38000	Alpes, F-38000	Alpes, F-38000	Alpes, F-38000
Grenoble, France	Grenoble, France	Grenoble, France	Grenoble, France
E-Mail:	E-Mail:	E-Mail:	E-Mail:
vincent.massavie@cea.fr	ghislain.despesse@cea.fr	sebastien.carcouet@cea.fr	xavier.maynard@cea.fr

Keywords

«Resonant inverter», «Power converter», «Piezoelectric component», «resonant frequency».

Abstract

This document introduces a new resonant inverter topology based on the Φ2 inverter. This new topology uses multiple resonance to pass fundamental and third harmonic at the switch terminals by filtering second harmonic with a piezoelectric component. This helps to reduce the voltage stress on the switch. Adding a piezoelectric resonator allows a better frequency stability and a better performance than a classic LC circuit. The structure and the design of the topology are described. Experimental results demonstrating the feasibility of the topology and a comparison with simulation results are done. The prototype works at 1.4MHz for an input voltage of 20V, an AC output voltage of 20V and an output power of 15W.

1) Introduction

Volume, weight and efficiency are major requirements of many modern power applications. Switching at high frequency allows answering to power density criteria by reducing exchanged energy per cycle and then the value and the size of passive components. The paper introduces a new topology of inverter, which uses a piezoelectric component to reduce the voltage stress on the switch. The frequency stability and the high quality factor of the piezoelectric resonator are very interesting characteristics for HF converters.

Section 2 develops the operating principle and the design of the inverter. Section 3 presents a validation of the design with simulations and experimental measurements for an inverter operating at 1.4MHz, with a DC input voltage of 20V, an AC output voltage of 20V and an output power of 15W. Additional tests are carried out experimentally by replacing the piezoelectric resonator with its equivalent in passive L-C components. Finally, section 4 concludes this work.

2) New topology of inverter: class L-Piezo

a) Working principle

The class L-piezo is a single transistor inverter but also a resonant Zero Voltage Switching (ZVS) topology. The components of the inverter are tuned to minimize the voltage stress across the transistor. It is closely related to the class Φ2 inverter of [1] [2], but the second harmonic filter is replaced by a piezoelectric component as illustrated in fig.1 .

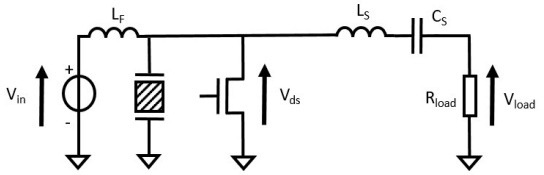


Fig.1 Class L-Piezo

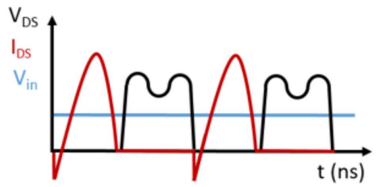


Fig.2 Voltage and current waveforms of class L-Piezo

This piezoelectric filter resonates at twice the switching frequency. It allows having a better stability in frequency and a better quality factor (>1000) than a LC circuit (<100). A piezoelectric resonator can decompose into an equivalent electric model around one of its resonant frequencies. Fig.3 shows the electrical model of a piezoelectric component operating around its resonant frequency as described in [3]&[6]. C_0 is the blocked capacity of the resonator, L_m, C_m and R_m are the motion branch, which are the electric representation of piezoelectric deformation.

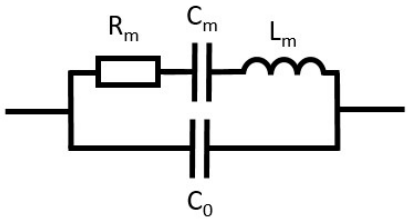


Fig.3 Electrical model of piezoelectric resonator

b) Methodology of design

- Characterization of piezoelectric resonator

The design of this inverter begins by the characterization of the piezoelectric resonator. The first variable to be fixed is the frequency f_r. It should be twice the switching frequency. It defines the piezoelectric size L_{xx} in the vibrational mode direction xx thanks to the frequency constant of piezoelectric material N_{xx} in the direction xx.

$$f_r = \frac{N_{xx}}{L_{xx}}$$

After this, the electrical model parameters of the Fig.3 can be deduced from piezoelectric material properties and sizes.

The blocked capacitance C_0 for a piezoelectric disc [4] is:

$$C_0 = \varepsilon_r . \varepsilon_0 . \frac{A}{t}$$

With:

- ε_0: vacuum permittivity ($\varepsilon_0 = 8.854 \times 10^{-12}$ F/m)
- A: electrode area (m²)
- ε_r: relative permittivity
- t: inter-electrode distance (m)

The coupling factor k_{xx} represents the quantity of electrical energy transformed into mechanical energy and vice versa, it is directly linked to the material property. From this coupling factor, the capacitance C_m can be deduced from C_0 [4].

$$C_m = k_{xx}^2 . C_0$$

By using the resonant frequency f_r, L_m can be calculated [4] :

$$L_m = \frac{1}{(2.\pi.f_r)^2.C_m}$$

Finally, the last component to calculate is R_m, representing the losses of the piezoelectric resonator. Based on the quality factor Q, R_m can be expressed by [4] :

$$R_m = \frac{(2.\pi.f_r).L_m}{Q}$$

- Design of output loop

The output loop designates components L_s, C_s and the load R_{load} show in Fig.1.

The load R_{load} can be calculated with the output power P_{load} and the output voltage V_{load}. V_{load} is an ac voltage with an amplitude equals to V_{in}, so the rms value of this voltage is $V_{load_eff} = \frac{V_{in}}{\sqrt{2}}$ and hence:

$$R_{load} = \frac{V_{in}^2}{2.P_{load}}$$

As the topology is close to the class Φ2 inverter [2], the same sizing equations can be used for this part. The LC circuit (L_s, C_s), has multiples functions: it is used as impedance divider with the load, as filter to keep only the fundamental of V_{ds} at the switching frequency, and it is also a dc blocking to obtain an ac voltage centered around 0V at the output.
In [2], the reactive interconnect X_s can be designed using the effective value of the fundamental component of V_{ds} voltage and the effective value of load voltage: $X_S = R_{load}.\sqrt{(\frac{V_{ds_eff}}{V_{ch_eff}})^2 - 1}$, with $V_{ds_eff} = \frac{4}{\pi.\sqrt{2}}.V_{in}$ and $V_{load_eff} = \sqrt{P_{load}.R_{load}}$

Afterward, L_s can be obtained by $L_S = \frac{X_S}{2.\pi.f_{switch}}$ and C_s with the resonance between L_s and C_s that must fit with the switching frequency.

- Input inductor and ZVS

The value of L_f is estimated by using the equation $L_f = \frac{1}{9.\pi^2.f_{switch}^2.C_0}$ which is detailed in [2], but this value is not very accurate.

This equation is a good starting point but the value obtained does not allow optimal operation of the inverter. In fact, a fine-tuning on the value of L_f is necessary, to have desired waveforms insuring the Zero Voltage Switching (ZVS) condition on the switch.

3) Validation of the design

To simulate this inverter, it was decided to take a real piezoelectric resonator and characterize it before integrating its parameters into the simulation. The choice of the resonator fell on a component from FUJI Ceramics [4]. It is a piezoelectric disc of Lead Zirconate Titanate (PZT) C-213 with a diameter of 25mm and a thickness of 0.75mm, same material as used for power conversion in [7] with the benefiting of a high k^2Q figure of merit (k_t=0.48 and Q=1280). For this application, we use the material in thickness mode, with a first thickness mode resonance of 2.8MHz. It filter the second harmonic on the transistor.

Based on the equations of the previous part and the datasheet values of the C-213 material and the material geometry, the estimated parameters of the piezoelectric resonator are:

Component	Value
L_m	1.53µH
C_m	2.11nF
R_m	215mΩ
C_0	9.16nF

Table I: Characterization of a PZT resonator by calculation

a) Validation of the piezoelectric model

A measurement with an impedance meter is done to validate the model of piezoelectric resonator around the resonant frequency.

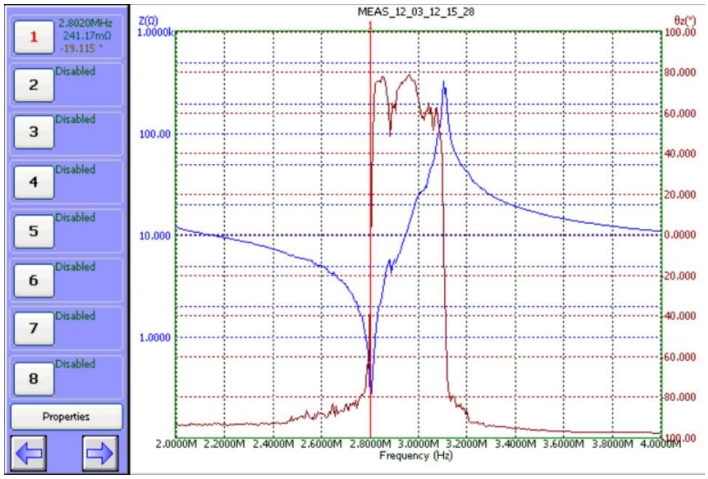


Fig.4 Impedance of a piezoelectric resonator around one of these resonant frequencies

To find capacitor C_0, we just measure the impedance at a point far from the resonance frequencies, where the impedance is capacitive $1/(C_0\omega)$.

At the resonant frequency, the LC branch impedance tends to zero, which allows us to measure the value of the resistance R_m.

$$R_m = Z(f_r)$$

Finally, C_m and L_m can be calculated using the resonant and antiresonant frequency:

$$C_m = C_0.\left(\left(\frac{f_a}{f_r}\right)^2 - 1\right) \qquad \text{and} \qquad L_m = \frac{1}{(2.\pi.f_r)^2.C_m}$$

To characterize the piezoelectric resonator, a WAYNE KERR 6500B impedance analyzer is used.

For the piezoelectric resonator selected, we obtain the following characteristics:

f_r = 2.80MHz $\qquad$ f_a = 3.12MHz $\qquad$ $Z(f_r)$ = 225 mΩ

The following values are therefore obtained for the characterization of the piezoelectric resonator:

Components	Values
L_m	1.6µH
C_m	2.02nF
R_m	241mΩ
C_0	8.6nF

Table II: Characterization of a PZT resonator by experimental measure

The values obtained by calculation and by measurement are very close, which validated the material parameters given by the manufacturer datasheet.

b) Simulation

A design of the inverter was done for a switching frequency of 1.4MHz, a dc input voltage of 20V, an ac output peak voltage of 20V and an output power of 15W. A LTSpice simulation have been made with these components values:

Components	Values
L_f	820nH
Piezoelectric resonator	Electrical model : C_0 = 8.6nF, L_m = 1.6µH, C_m = 2.02nF and R_m = 225mΩ
L_s	1.2µH
C_s	10nF
Switch	GaN model of GaN Systems : GS61004B
R_{load}	18Ω

Table III: List of component for the 1.4MHz L-Piezo inverter with V_{in} = 20V, f_s=1.4MHz and P_{load}=15W

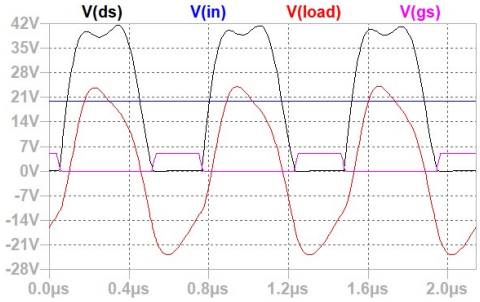


Fig.5 Voltage waveforms of class L-Piezo

The simulation presented in Fig.5 shows that the maximal value of drain-source voltage (V_{ds}) is 42V, that corresponds to twice the input voltage V_{in}. The load voltage is an ac voltage between 24V and -24V. The voltage V_{gs} (0-5V) commands the inverter. The Fig.5 shows that the inverter operate in ZVS to limit the losses in the switch.

The simulation shows that a class L-piezo can be functional and efficient even if some parameters are fixed by the piezoelectric material properties, like the ratio of C_m/C_0, which is limited by the coupling factor of the material.
In the next part, we propose to check experimentally the good operation of this L-piezo converter.

c) Experimental results

The L-Piezo inverter was implemented on a two layer PCB made in CEA Grenoble and using a C213 FUJI piezoelectric resonator, the transistor reference is GS61004B from GaN Systems [5], inductors and capacitors are from WURTH.

Components	manufacturers	References
L_f	WURTH	74477450082
Piezoelectric resonator	FUJI ceramics	C213
Transistor GaN	GaN Systems	GS61004B
L_{s12}	WURTH	74437356010 744373560022
C_s	WURTH	885012206089
Driver	Microchip Technology	TC4422AVOA

Table IV: List of references for experimental class L-Piezo

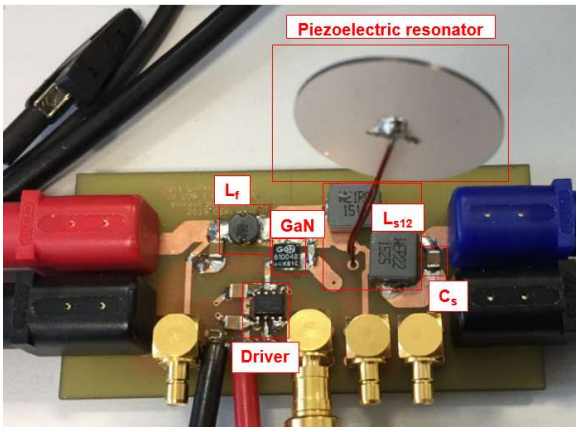


Fig.6 Experimental class L-Piezo inverter

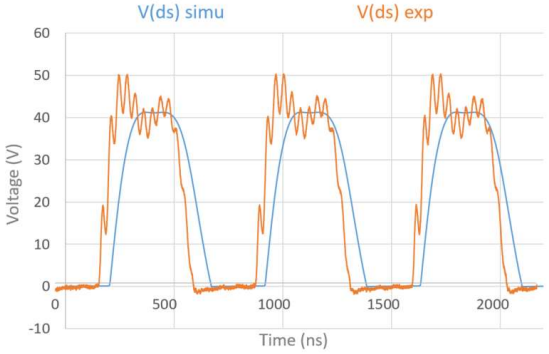


Fig.7 Simulate and experimental waveforms of drain to source voltage (V_{ds})

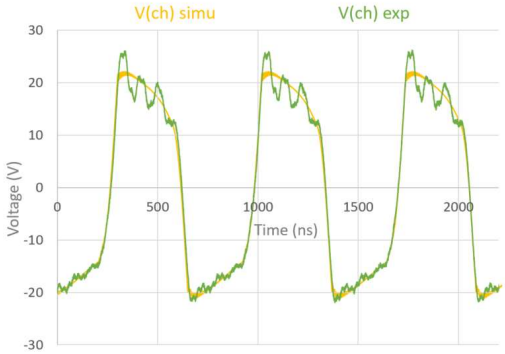


Fig.8 Simulated and experimental waveforms of load voltage of inverter stage (V_{load})

As shown in Fig.7 and Fig.8, the drain to source voltage (V_{ds}) and the output voltage of inverter stage (V_{load}) waveforms are in good agreement with simulation waveforms. The maximum value across the GaN switch is 50V. The parasitic ripples on the GaN voltage (V_{ds}) and in the output voltage (V_{load}) is a strong harmonic that look to be produced by the parasitic inductance of the wires that connect the resonator to the electronic board.

In the following part, we propose to compare our L-piezo inverter with a conventional class Φ2 inverter. The components of the conventional class Φ2 inverter are sized in order to have a similar behavior.

d) Comparison between L-Piezo and an artificial L-Piezo made with L-C passive filter

To complete the study of this new converter, we compare its performance by replacing the piezoelectric resonator with its equivalent in L-C passive components.
The goal is the comparison between an L-C passive filter and a piezoelectric filter.

Equivalent L-C components	Values	Manufacturers	References
L_m	1.6µH	WURTH	74405031015
C_m	2.02nF	KEMET	C0805C202J1GACTU
C_0	8.6nF	TDK	CGA3E1C0G2A822J080AE

Table V: List of references for equivalent L-C component

As for the simulation, it was carried out by including the losses of all the components included in Table II using the model spice provided by the manufacturers. However, the losses due to the parasitic inductance of the circuit and connections are not taken into account in the simulation.
The input voltage has an effect on the output power, so the efficiency was calculated for different values of V_{in}.

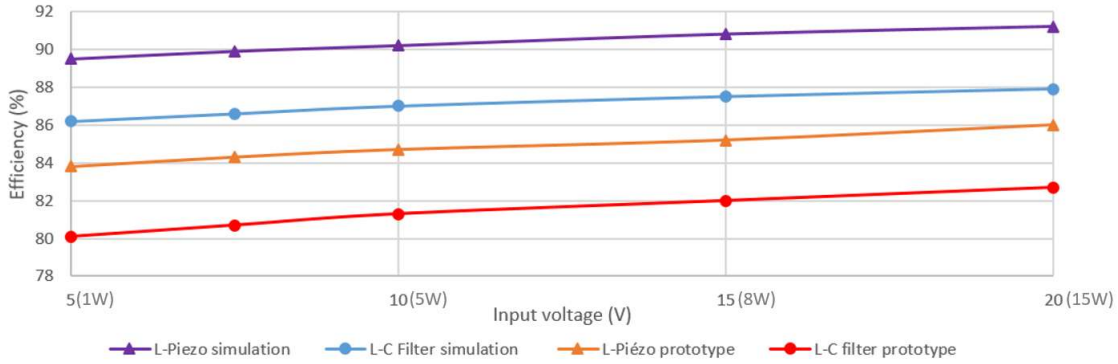


Fig.9 Efficiency comparison between L-Piezo simulation, L-C filter simulation, L-Piezo prototype and L-C filter prototype in the $5V \leq V_{in} \leq 20V$ range

At nominal input voltage (20V), with an output power of 15W, the efficiency of the complete L-Piezo inverter is 86.05%, lower than the simulation (91.19%) because some losses are not taken into account in the simulation such as parasitic elements of the PCB, connection losses or the thermal effect on the components.
All the four efficiency curves have the same shape. However, the L-piezo has a better efficiency than its equivalent L-C filter (83.08%). This performance gain is due to the piezoelectric material having a high quality factor compared to a conventional LC circuit. Indeed, inductances have a low quality factor which penalize the global quality factor of the L-C filter (Q_{piezo}= 1280, Q_{Lm}= 55). This can be confirmed by the fact that the gap between the two simulations and the two prototypes is the same. These results validate the initial hypothesis concerning HF converters incorporating piezoelectric materials.

4) DC/DC converter

To push the topology further, a rectifier has been added to obtain a DC / DC converter.

a) Class DE rectifier

The chosen rectifier is a class DE resonant rectifier [8] [9]; its circuit is shown in fig.10. This rectifier is a zero voltage switching rectifier topology with a low diode voltage stress.

When the diode D_1 is in conduction, the C_c capacitor is charging and a DC voltage appears across it. Afterward, D2 goes into conduction and charge the filter capacitor C_{out}. C_c and C_{out} have a large value so their impedance is negligible at 1.4MHz. Schottky diodes are chosen for D_1 and D_2 in order to avoid reverse recovery losses. The shunt inductor L_a resonates with diodes junction capacitances (C_{d1} and C_{d2}) at the switching frequency. The goal is to obtain an equivalent global resistive impedance. The output voltage of this rectifier is equal to the pic-to-pic of the AC input voltage.

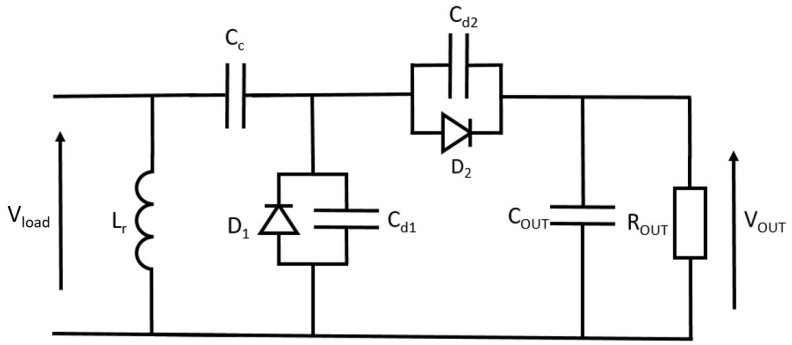


Fig.10 Class DE rectifier

The Fig.11 and Fig.12 show the current and voltage waveforms of this rectifier. The maximum diode voltage stress is equal to twice the maximum of AC input voltage (here 40V), which is the value of rectifier output voltage.

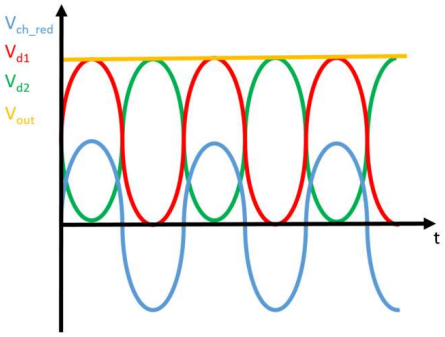


Fig.11 Voltage waveforms of class DE rectifier

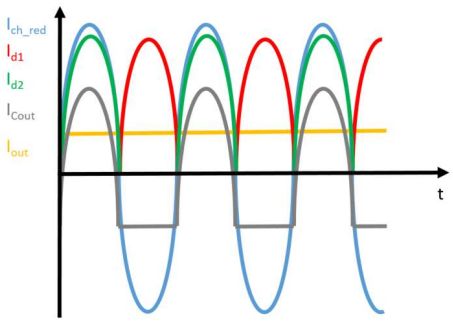


Fig.12 Current waveforms of class DE rectifier

b) Matching network

The class L-Piezo inverter work with a fixed resistive load. The class DE rectifier has a global resistive impedance but the value of this impedance is not the same as the inverter load. Therefore, a matching network is necessary to obtain a good working of the DC/DC converter [10].

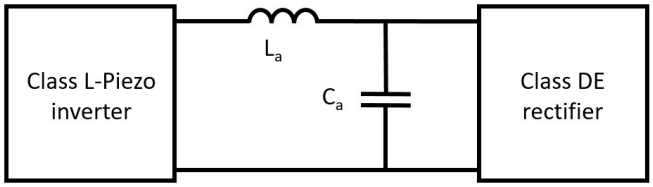


Fig.13 Matching network

In Fig.13, the inductance L_a is calculated to have a global rectifier impedance equal to the load inverter. The capacitor C_a, resonates with L_a at the switching frequency, which allows the matching network to have a resistive impedance.

c) Experimental results on the full DC/DC converter

Input voltage and input current waveforms of the class DE rectifier are shown in fig.14. The resistive behavior of the class DE is highlighted by the fact that the input voltage and current are in phase.

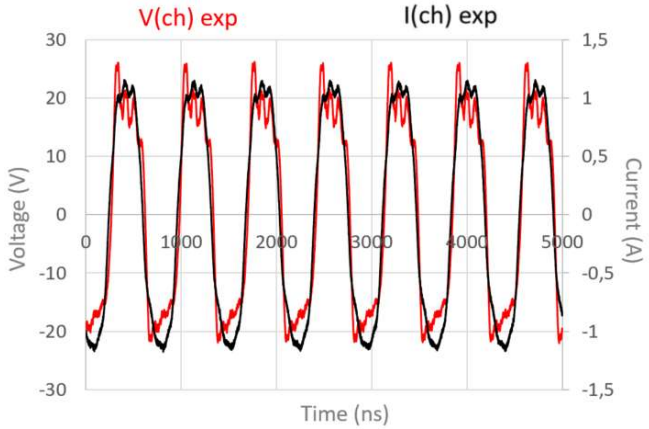


Fig.14 Input voltage and input current of the experimental rectifier

Diodes use for the class DE rectifier are VS-8TQ080S-M3 schottky diodes from Vishay. As visible on Fig 15, the converter output voltage has a similar value to the one simulated.

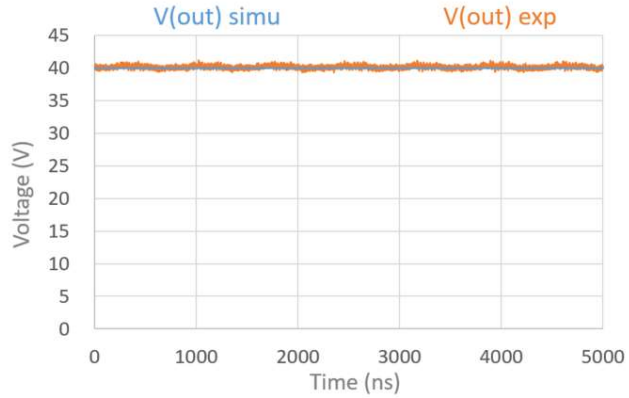


Fig.15 Simulate and experimental waveforms of output voltage (V_{out})

At 20V input, the efficiency of the class DE rectifier is 90%, so the global efficiency of the full DC/DC converter at nominal input voltage is 77.4%.

5) Conclusion

This document presents a new resonant inverter, that we call L-Piezo inverter. It takes advantage of the frequency stability and the high quality factor of a piezoelectric resonator to filter the second harmonic of the Φ2 inverter. This allows to obtain a ZVS inverter with low semiconductor voltage stress.
The structure of the proposed topology is described, and a design procedure is introduced. Experimental results demonstrating the good operation of the new L-Piezo topology are also presented for a 1.4MHz, 20V, 15W converter. The waveforms provide by the experimental tests are closed to the one obtained in simulation and it validate the feasibility of the topology. The replacement of the piezoelectric resonator by its equivalent in passive component shows the importance of having a high quality factor to reduce the losses. This topology can be adapted to make a DC/DC converter by adding a suitable rectifier. A better integration for the resonator on the PCB can be done to reduce the parasite inductance and losses. In perspective, we aim to rise the input voltage and the switching frequency of the converter.

References

[1] O. Leitermann, « Radio frequency dc-dc converters : device characterization, topology evaluation, and design », Thesis, Massachusetts Institute of Technology, 2008.

[2] J. M. Rivas, Y. Han, O. Leitermann, A. Sagneri, et D. J. Perreault, « A High-Frequency Resonant Inverter Topology with Low Voltage Stress », in *2007 IEEE Power Electronics Specialists Conference*, juin 2007, p. 2705-2717, doi: 10.1109/PESC.2007.4342446.

[3] K. S. V. Dyke, « The Piezo-Electric Resonator and Its Equivalent Network », *Proc. Inst. Radio Eng.*, vol. 16, nº 6, p. 742-764, juin 1928, doi: 10.1109/JRPROC.1928.221466.

[4] « piezoelectric ceramics ». http://www.fujicera.co.jp/managed/wp-content/themes/fujicera/digitalbook/en/elements/index_h5.html#12 (consulté le nov. 09, 2020).

[5] « GS61004B », *GaN Systems*. https://gansystems.com/gan-transistors/gs61004b/

[6] B. Pollet, G. Despesse and F. Costa, "A New Non-Isolated Low-Power Inductorless Piezoelectric DC–DC Converter," in IEEE Transactions on Power Electronics, vol. 34, no. 11, pp. 11002-11013, Nov. 2019, doi: 10.1109/TPEL.2019.2900526.

[7] M. Touhami, G. Despesse and F. Costa, "A New Topology of DC-DC Converter Based On Piezoelectric Resonator" presented at IEEE COMPEL 2020, Nov. 2020.

[8] Y. Minami et H. Koizumi, « Class DE current driven low di/dt rectifier », in *2014 IEEE International Symposium on Circuits and Systems (ISCAS)*, juin 2014, p. 105-108, doi: 10.1109/ISCAS.2014.6865076.

[9] T. Misawa, K. Fukui, et H. Koizumi, « Zero current switching Type Class DE rectifier », in *IECON 2012 - 38th Annual Conference on IEEE Industrial Electronics Society*, oct. 2012, p. 858-863, doi: 10.1109/IECON.2012.6388735.

[10] R. Makhoul *et al.*, « A DC/DC Converter Based on a Very High Frequency Tuned Power Oscillator », in *PCIM Europe 2019; International Exhibition and Conference for Power Electronics, Intelligent Motion, Renewable Energy and Energy Management*, mai 2019, p. 1-6.